Proceedings of the DIS'2004, Štrbské Pleso, Slovakia

AN NLO QCD ANALYSIS OF INCLUSIVE CROSS-SECTION DATA AND JET PRODUCTION DATA FROM THE ZEUS EXPERIMENT AT HERA-I

A M COOPER-SARKAR
Denys Wilkinson Building
Oxford University Physics Department
1 Keble Rd, Oxford OX1 3RH, UK
E-mail: a.cooper-sarkar@physics.ox.ac.uk

The ZEUS inclusive differential cross-section data from HERA-I, for charged and neutral current processes taken with e^+ and e^- beams, have been used in a new a NLO QCD analysis to extract the parton distribution functions (PDFs) of the proton within a single experiment. The precision of the high-x gluon determination is improved by using ZEUS differential cross-section data on inclusive jet production in e^+p scattering and di-jet production in γp scattering.

1 Introduction

ZEUS data from HERA-I on neutral and charged current (NC and CC) e^+p and e^-p cross-sections [1,2,3,4,5,6] have been used in a NLO QCD DGLAP analysis in order to determine the parton distributions functions (PDFs) using data from within a single experiment. PDF determinations are usually global fits [7,8,9], which use fixed target DIS data as well as HERA data. In such analyses, the high statistics HERA NC e^+p data, which span the range $6.3 \times 10^{-5} < x < 0.65, 2.7 < Q^2 < 30,000\text{GeV}^2$, have determined the low-x sea and gluon distributions, whereas the fixed target data have determined the valence distributions and the higher-x sea and gluon distributions. The most important inputs for determining the valence distributions have been the ν-Fe and the μD fixed target data, but these data sets suffer from uncertainties due to heavy target corrections [10]. In the present analysis the ZEUS high Q^2 cross-section data [2,3,4,5,6] are used to determine the valence distributions thus eliminating such uncertainties. PDF fits to DIS data alone have suffered from a lack of information on the high-x gluon. In the present analysis ZEUS jet production data are used to constrain the gluon PDF.

The PDFs are presented with full accounting for uncertainties from correlated systematic errors (as well as from statistical and uncorrelated sources). Peforming an analysis within a single experiment has considerable advantages in this respect, since the global fits have found significant tensions between different data sets, which make a rigorous statistical treatment of uncertainties difficult.

2 Analysis

The kinematics of lepton hadron scattering is described in terms of the variables Q^2, the invariant mass of the exchanged vector boson, and Bjorken x, the fraction of the

© Institute of Experimental Physics SAS, Košice, Slovakia

momentum of the incoming nucleon taken by the struck quark (in the quark-parton model). The differential cross-sections for the NC and CC processes are given in terms of structure functions which are directly related to quark distributions. The Q^2 dependence of these structure functions is predicted by perturbative QCD. At $Q^2 \lesssim 1000\text{GeV}^2$ the NC structure function F_2 dominates the charged lepton-hadron cross-section and for $x \lesssim 10^{-2}$, F_2 itself is sea quark dominated whereas its Q^2 evolution is controlled by the gluon contribution, such that ZEUS data provide crucial information on quark and gluon distributions. At high Q^2, the NC structure function xF_3 becomes increasingly important, and gives information on valence quark distributions. The CC interactions also enable us to separate the flavour of the valence distributions at high-x. For a full explanation of the relationships between DIS cross-sections, structure functions, PDFs and the QCD improved parton model see for example ref. [12]. The present analysis is performed within the conventional paradigm of leading twist, NLO QCD, with the renormalisation and factorization scales chosen to be Q^2. The QCD predictions for the structure functions are obtained by solving the DGLAP evolution equations at NLO in the $\overline{\text{MS}}$ scheme. These equations yield the PDFs at all values of Q^2 provided they are input as functions of x at some input scale Q_0^2. The resulting PDFs are then convoluted with coefficient functions, to give the structure functions which enter into the expressions for the cross-sections. These coefficient functions are calculated using the general mass variable flavour number scheme of Roberts and Thorne [11] for heavy quark production.

The PDFs for u valence, d valence, total sea, and gluon are each parametrized by the form

$$p_1 x^{p_2} (1-x)^{p_3} (1+p_4 x)$$

at $Q_0^2 = 7\text{GeV}^2$. No advantage in χ^2 results from using more complex polynomial forms. The normalisation parameters p_1 for the d and u valence and for the gluon are constrained to impose the number sum-rules and momentum sum-rule. The p_2 parameter which constrains the low-x behaviour of the u and d valence distributions is set equal, since there is no information to constrain any difference. When fitting to ZEUS inclusive cross-section data alone it is necessary to constrain some of the parameters which control the high-x sea and gluon shapes, because HERA-I data do not have high statistics at large-x, in the region where these distributions are small. There are two possible strategies towards making these constraints.

Firstly, the focus is on the valence distributions and the number of free parameters describing the high-x sea and gluon is restricted. There are various ways to make restrictions. One possibility is to set $p_4 = 0$ for both these distributions. However this does not allow any structure at medium x for Q^2 near the input scale. Alternatively, the p_4 parameters can be freed but the p_3 parameters fixed to the values obtained in the ZEUS global fit [9]. In this case, model uncertainties on the high-x sea and gluon PDFs must include the effect of changing these fixed values of p_3 within the limits of their errors as determined in the global fit. In practice there is very little difference in the shapes and errors on the sea and gluon PDFs determined by these two ways of making restrictions. Distributions are presented for the latter choice. This fit has 10 free parameters and is called the ZEUS-O fit.

Secondly, a more ambitious strategy is pursued. ZEUS data on jet production are included in the PDF fit. This not only gives more information on the high-x gluon PDF, but also establishes that NLOQCD is able to simultaneously describe inclusive cross-sections and jet cross-sections providing a compelling test of QCD factorization. This fit is called the ZEUS-JETS fit. The method of incorporating the jet production data in the fit is discussed in detail in Sec. 3.2

For both analyses the strong coupling constant is fixed to $\alpha_s(M_Z^2) = 0.118$ and the following cuts are made on the data: (i) $W^2 > 20\text{GeV}^2$ to reduce the sensitivity to target mass and higher twist contributions which become important at high x and low Q^2; (ii) $Q^2 > 2.5\text{GeV}^2$ to remain in the kinematic region where perturbative QCD should be applicable. Full account has been taken of correlated experimental systematic errors by the Offset Method, as decribed in the previous ZEUS analysis [9] and discussed extensively in [14]. Further details of the analysis may be found in [15]

3 Results

3.1 ZEUS-O fit results

For the ZEUS-O fit, inclusive cross-section data from 112 pb^{-1} of HERA-I running are used. A good description of cross-section data over the whole range of Q^2 from 2.5 to 30000 GeV^2 is obtained. The χ^2 is 386 for 509 data points. The quality of the fit to the high-Q^2 reduced cross-section data is illustrated in Fig. 1.

The valence distributions are shown in Fig 2. Although the high-x valence distributions are not quite as well constrained as they are in global fits including fixed target data [9,7,8] they are becoming competitive, particularly for the less well known d-valence distribution. Furthermore, they are free from uncertain heavy target corrections.

The gluon and sea distributions are shown in Fig. 2. They exhibit the familiar features of the sea rising at low-x down to surprisingly low Q^2 values, and the gluon flattening and then becoming valence-like in the same kinematic region. They are as well determined as the corresponding distributions of the global fits [9,7,8] at low-x, since the ZEUS data were crucial in determining these distributions for all the fits. At high-x they have the same uncertainties as the global fits because of the constraints that have been applied.

The experimental errors represent the most significant source of uncertainty on these distributions. Variation of analysis choices, such as the value of Q_0^2, the minimum Q^2 of data entering the fit, and changing the form of the parametrization at Q_0^2, do not produce a large model uncertainty.

3.2 ZEUS-JETS fit results

The gluon PDF contributes only indirectly to the inclusive DIS cross-sections. However it makes a direct contribution to jet cross-sections through the Boson-Gluon-Fusion process. In the present analysis the mid to high-x gluon distribution is constrained by including in the fit two ZEUS measured jet cross sections:

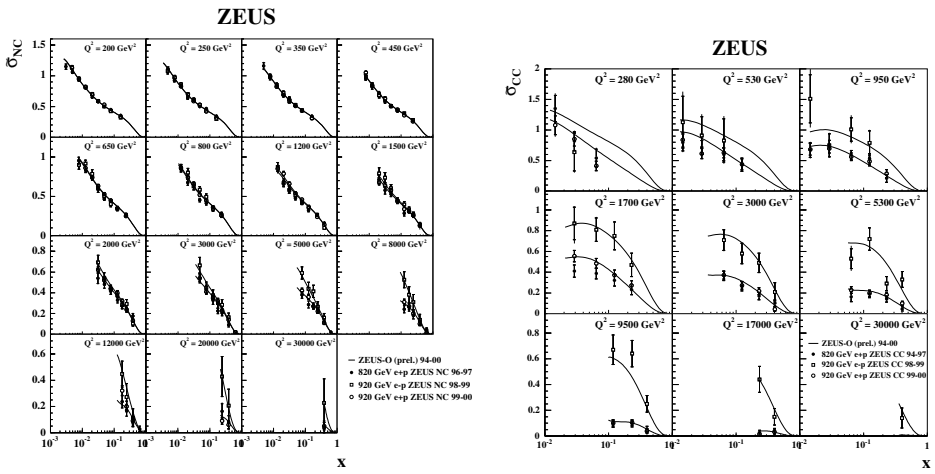

,

Figure 1. Left plot: ZEUS-O fit to high Q^2 NC data. Right plot: ZEUS-O fit to high Q^2 CC data.

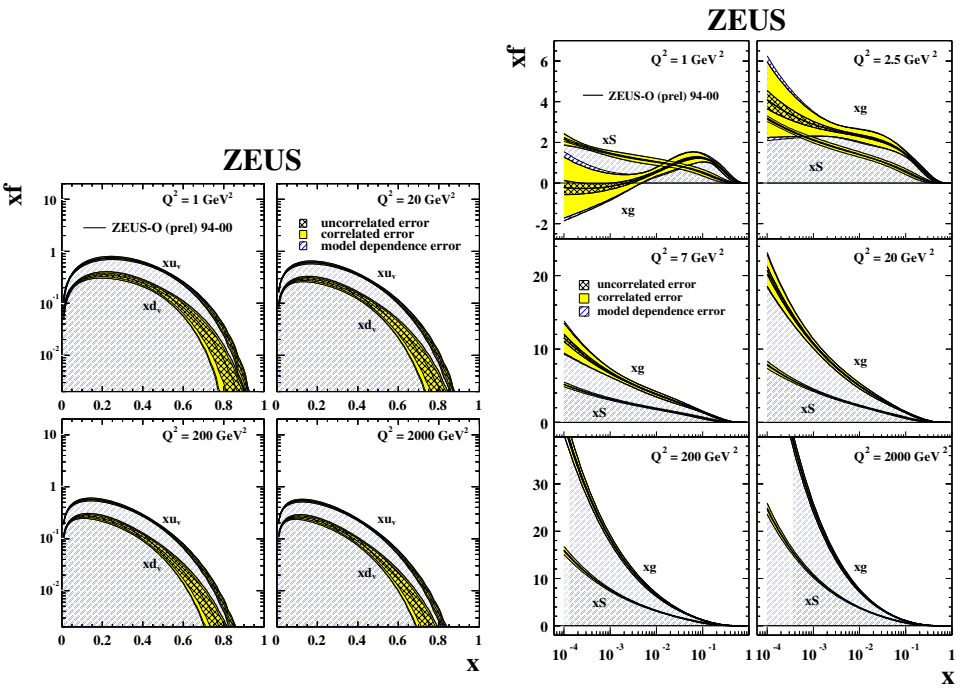

,

Figure 2. Left plot: Valence PDFs extracted from the ZEUS-O fit. Right plot: Gluon and sea PDFs extracted from the ZEUS-O fit.

- 30 data points from six DIS inclusive jet differential cross-sections as a function of the transverse energy, E_T^B, in the Breit frame, for different Q^2 bins [16].
- 38 data points from six direct photoproduction di-jet cross-sections as a function of the transverse energy of the most energetic jet, E_T^{jet1} in the lab, for different jet rapidity ranges [17].

For each of these data sets the calorimeter energy scale uncertainty and the normalization uncertainty have been treated as correlated systematic errors.

The programme of Frixione and Ridolfi [18] is used to compute NLO QCD cross sections for photoproduced di-jets and DISENT [19] is used to compute NLO QCD cross sections for jet production in DIS. These programmes are too slow to be used every iteration of a fit. Thus these codes are used to produce grids,in ξ (the parton momentum fraction) and μ_F^2 (the factorization scale), of weights which represent sub-process cross-sections for each flavour of parton (gluon, up-type, down-type). This is done for each cross-section bin and these weights are then used to reconstruct the cross-sections as follows

$$d\sigma(jets) = \sum_{a=u,d,g} \int\int d\xi d\mu_F^2 f_a(\xi,\mu_F^2)\sigma_a(\xi,\mu_F^2,\alpha_s(\mu_R)) \qquad (1)$$

where f_a is the PDF for parton type a at parton momentum fraction ξ and scale μ_F, and σ_a is the sub cross-section weight. The factorization scale is chosen as $\mu_F = Q$ for the DIS jets, and the renormalization scale is $\mu_R = E_T$ (with $\mu_R = Q$ as a cross-check). For the photoproduced di-jets the standard scale choices are $\mu_R = \mu_F = E_T/2$ (where E_T is the summed E_T of final state partons). The grids reproduce the NLO predictions to better than 0.5%. The predictions are then multiplied by hadronization corrections and Z_O corrections before they are fitted to data.

The predictions for photoproduced jets can obviously be influenced by the choice of the input photon PDF. Thus the analysis is restricted to direct photoproduction, defined such that all data points satisfy $x_\gamma^{OBS} > 0.75$, where x_γ^{OBS} is a measure of the fraction of the photon's momentum which enters into the hard scattering, see ref. [17]. This minimizes sensitivity to the choice of the photon PDF. The AFG photon PDF is used to make the standard predictions, and the GRV photon PDF is used as a cross-check. There is no visible difference to the extracted proton PDFs.

The jet data are input to fits in which the p_3 and the p_4 parameters, which control the high-x behaviour of the sea and the gluon PDF, are freed. It is found that these data constrain the gluon distribution in the range $0.01 < x < 0.1$. However, the sea distribution is not significantly constrained, so that the strategy of fixing one of the high-x sea parameters is retained. Thus the ZEUS-JETS fit has 11 free parameters. The fit χ^2 is 479 for 577 data points. The quality of the fit to the jet data is illustrated in Fig 3.

Fig. 4 compares the gluon distribution and its errors for 11 parameter fits including and not including the jet data. Although the jet data constrain the gluon directly only in the range $0.01 \lesssim x \lesssim 0.1$, the momentum sum-rule ensures that the indirect constraint of this data is still significant at higher x. The decrease in the uncertainty on the gluon distribution is striking, even up to high Q^2.

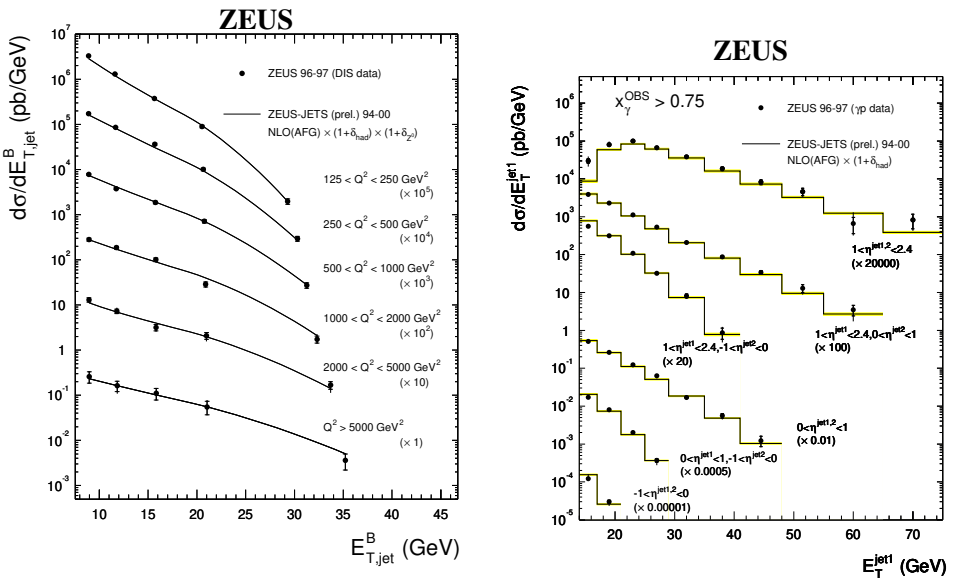

Figure 3. Left plot: ZEUS-JETS fit to DIS jet data. Right plot: ZEUS-JETS fit to direct photo-produced dijet data.

Fig. 5 (left hand plot) compares all the PDFs for ZEUS-O and ZEUS-JETS fits, illustrating that the valence and sea PDFs are not significantly influenced by the input of the jet data. The PDFs from the previous ZEUS-S global fits [9] and the MRST and CTEQ PDFs [7,8] are also shown on this figure. There is good agreement between all the ZEUS PDF extractions. The CTEQ and MRST PDFs are also compatible considering the size of the PDF uncertainties.

References

1. ZEUS Collab., S Chekanov *et al.* , *Eur. Phys. J.* C **21** 443 (2001).
2. ZEUS Collab., J Breitweg *et al.* , *Eur. Phys. J.* C **12** 411 (2000).
3. ZEUS Collab., S Chekanov *et al.* , *Eur. Phys. J.* C **28** 175 (2003).
4. ZEUS Collab., S Chekanov *et al.* , *Phys. Lett.* B **539** 197 (2002).
5. ZEUS Collab., S Chekanov *et al.* , DESY-03-214, hep-ex/0401003.
6. ZEUS Collab., S Chekanov *et al.* , *Eur. Phys. J.* C **32** 16 (2003).
7. A D Martin *et al.* , *Eur. Phys. J.* C **23** 73 (2002), *Eur. Phys. J.* C **28** 455 (2003).
8. J Pumplin *et al.* ,*JHEP* **0207** 012 (2002).
9. ZEUS Collab., S Chekanov *et al.* , *Phys. Rev.* D **67** 0120071 (2003).
10. A M Cooper-Sarkar *et al.* , *J. Phys.* G. **25** 1387 (1999).
11. R G Roberts and R S Thorne, *Phys. Rev.* D **57** 6871 (1998).

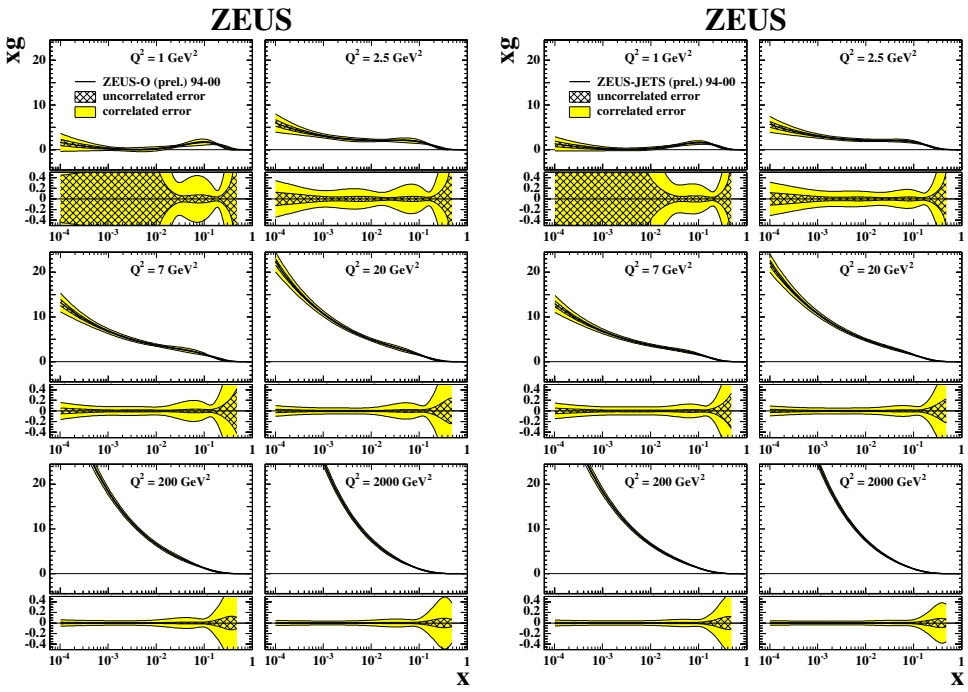

,

Figure 4. Left plot: Gluon distributions extracted from an 11-parameter PDF fit excluding jet production data. Right plot: Gluon distributions extracted from the an 11-parameter PDF fit including jet production data (ZEUS-JETS fit). The uncertainties on these distributions are shown beneath each distribution as fractional differences from the central value. Note that model uncertainty is not visible for these fits

12. R C E Devenish and A M Cooper-Sarkar, 'Deep Inelastic Scattering', OUP 2004, Chapter 6.
13. Particle Data Group, S Eidelman *et al.* , *Phys. Lett.* B **592** 1 (2004).
14. A M Cooper-Sarkar, *J. Phys.* G. **28** 2609 (2002), R S Thorne *et al.* , *J. Phys.* G. **28** 2717 (2002).
15. ZEUS Collab.,Paper 5-0294, Internationla Conference on High Energy Physics, Beijing, 2004
16. ZEUS Collab., S Chekanov *et al.* , *Phys. Lett.* B **547** 164 (2002).
17. ZEUS Collab., S Chekanov *et al.* , *Eur. Phys. J.* C **23** 615 (2002).
18. S Frixione and G Ridolfi, *Nucl. Phys.* B **507** 315 (1997).
19. S Catani and M H Seymour, *Nucl. Phys.* B **485** 291 (1997).
20. H1 Collab.,C Adloff *et al.* , *Eur. Phys. J.* C **30** 1 (2003).

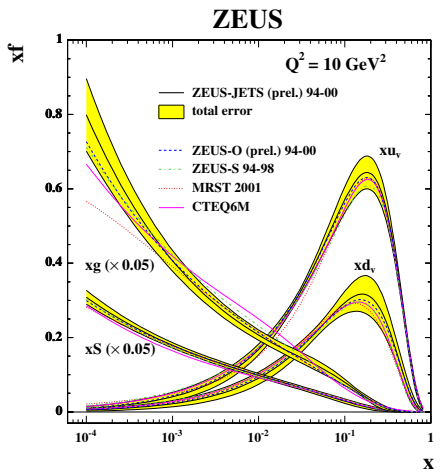

Figure 5. PDFs extracted from the new ZEUS-O and ZEUS-JETS fits compared to the previous ZEUS-S analysis and the MRST and CTEQ PDFs.